AIAA JOURNAL
Vol. 45, No. 3, March 2007

On the Perception of Crackle in High-Amplitude Jet Noise

Kent L. Gee*
Brigham Young University, Provo, Utah 84602
and
Victor W. Sparrow,† Anthony Atchley,‡ and Thomas B. Gabrielson§
Pennsylvania State University, University Park, Pennsylvania 16802

DOI: 10.2514/1.26484

Crackle is a phenomenon sometimes found in supersonic jet noise and can comprise an annoying and dominant part of the overall perceived noise. In the past, crackle has been commonly quantified by the skewness of the time waveform. In this investigation, a simulated waveform with a virtually identical probability density function and power spectrum as an actual F/A-18E afterburner recording has been created by nonlinearly transforming a statistically Gaussian waveform. Although the afterburner waveform crackles noticeably, playback of the non-Gaussian simulated waveform yields no perception of crackle at all, despite its relatively high skewness. Closer examination of the two waveforms reveals that although they have virtually identical statistics, there are considerable differences in their time rates of change in the intense compressive portions of the waveforms. The afterburner waveform is much more shocklike with its more rapid variations in pressure than the non-Gaussian simulated waveform. This results in a significant difference in the probability distributions of the time derivatives of the actual and simulated data and suggests that the perception of crackle in jet noise waveforms may be better quantified with statistics of the time derivative of the waveform, rather than by the skewness of the time waveform itself.

Nomenclature

E	=	quadratic cost function to be minimized
$g(x)$	=	nonlinear transformation function
K	=	kurtosis, $K = \langle (x-M)^4 \rangle / \sigma^4$
M	=	mean of the time series, $M = \langle x \rangle$
S	=	skewness, $S = \langle (x-M)^3 \rangle / \sigma^3$
V	=	variance, $V = \langle (x-M)^2 \rangle$
$x(t)$	=	Gaussian time series
$y(t)$	=	non-Gaussian time series generated by $y = g(x)$
σ	=	standard deviation of the time series
$\langle\rangle$	=	expectation operator

I. Introduction

THE phenomenon known as "crackle" that sometimes occurs in supersonic jet noise has been described as a particularly annoying and dominant component of the overall noise [1,2]. However, relatively few studies of the characteristics of crackle have been carried out. In 1975, Ffowcs Williams et al. [1] published what remains the seminal paper on the subject. They describe crackle as "sudden spasmodic bursts of a rasping fricative sound not dissimilar to that made by the irregular tearing of paper.... It is a startling staccato of cracks and bangs and its onomatope, 'crackle,' conveys a subjectively accurate impression." One of the main conclusions of Ffowcs Williams et al., a conclusion that has guided investigations since then, was that the skewness of the time series is an important parameter in determining when a jet is or is not crackling. The skewness, which is a normalized form of the third central moment of the probability density function (PDF) of the time waveform, is a measure of the asymmetry of the PDF. (Note that a Gaussian PDF has skewness of zero.) Based on examination of various jet noise recordings, Ffowcs Williams et al. used the skewness to establish a threshold for the existence of crackle in a waveform. They reported that waveforms for which $S > 0.4$ "distinctly" crackle and waveforms for which $S < 0.3$ do not. The behavior of crackle for $0.3 < S < 0.4$ was not defined, but likely can be taken to mean the region in which the perception of crackle is present but not "distinct" or the region in which crackle is only present in some recordings.

More recently, Krothapalli et al. [2] and Petitjean and McLaughlin [3] have looked into the origin and the nature of crackle and have made measurements of the skewness of model-scale jets. McInerny [4] has performed extensive statistical analyses of the noise signatures from rocket launches and shown that the waveforms are substantially skewed. Measurements of skewness have also been reported for full-scale military jet aircraft noise at close range. A recent study [5] of the propagation of noise from a tied-down military jet aircraft has shown that the F/A-18E time series at 18 m (60 ft) and at afterburner (AB) has a skewness value of $S = 0.60$ at the peak emission angle. The measured waveform with the same aircraft at military (Mil) power has a skewness of $S = 0.38$ at 18 m, again at the peak emission angle. Because the skewness for the AB recording clearly exceeds the $S > 0.4$ threshold suggested by Ffowcs Williams et al. [1], and the skewness for the Mil recording is essentially equal to it, the perception of crackle should be noticeable in both time series. Playback of both the AB and Mil recordings confirms this hypothesis.

However, an impulsivelike quality similar to crackle has been noted by the authors in certain time waveforms from propagation measurements where S is well below the Ffowcs Williams et al. threshold (e.g., $S < 0.15$). According to the $S > 0.4$ criterion, these waveforms should be crackle free. It has further been noted that this cracklelike quality of the noise at large distances appears to be linked to cases where nonlinearity plays a significant role in the propagation [6]. These observations have prompted this study of the cause of the *perception* of an impulsive or cracklelike quality in certain jet noise waveforms. It is stressed at the outset that the focus of this investigation is not on the physical mechanisms responsible for the generation of a skewed waveform near the source. Rather, this study addresses the question of whether significant skewness by itself is

Presented as Paper 2530 at the 12th AIAA/CEAS Aeroacoustics Conference, Cambridge, MA, 8–10 May 2006; received 11 July 2006; revision received 20 September 2006; accepted for publication 4 November 2006.

*Assistant Professor, Department of Physics and Astronomy, N319 ESC; kentgee@byu.edu. Member AIAA.

†Associate Professor, Graduate Program in Acoustics, 202 Applied Science Building; vws1@psu.edu. Senior Member AIAA.

‡Professor of Acoustics and Chair, Graduate Program in Acoustics, 217 Applied Science Building; atchley@engr.psu.edu. Member AIAA.

§Senior Research Associate Scientist, Applied Research Lab, P.O. Box 30, State College, PA 16804; tbg3@psu.edu.

sufficient to cause a listener to perceive crackle in a waveform. The answer to this question has direct implications regarding the suitability of skewness as a quantifier of crackle.

To examine the effect of skewness on the perception of crackle, methods of creating non-Gaussian waveforms have been studied. The process selected to generate skewed waveforms for the purposes of investigating crackle is first described. This description is followed by a summary of results regarding skewed waveforms that have been created to simulate actual jet noise waveforms that crackle. Finally, findings from additional analysis of the waveforms' attributes are presented and discussed.

II. Non-Gaussian Waveform Simulation Theory

To systematically study how skewness affects the perception of crackle, it is necessary to have a means of generating non-Gaussian (e.g., skewed) waveforms. It is desired that these non-Gaussian waveforms possess more than simply the same skewness as actual jet noise data because a single moment of the PDF does not uniquely specify a probability distribution. The waveforms should have, in particular, the same mean, variance, skewness, and kurtosis as the measured jet noise data, in addition to having the same spectrum. Specification of these four moments of the PDF, which are defined in the nomenclature, makes possible the generation of a simulated waveform with a virtually identical PDF as the measured waveform. The underlying theory of non-Gaussian waveform generation and its implementation are now discussed. The theoretical discussion is largely after the manner of Bendat [7].

A zero-memory nonlinear system may be defined as a system that acts on the present input in a nonlinear fashion. Correspondingly, a non-Gaussian waveform, $y(t)$, may be generated by passing a statistically Gaussian signal, $x(t)$, through a zero-memory nonlinear transformation function (NTF), denoted as $y = g(x)$. It is noted that although x varies as a function of time, $g(x)$ is time invariant. As an example, a quadratic zero-memory NTF, similar to that used to model a hardening-softening nonlinear spring [7], may be written as

$$y = g(x) = a + bx + cx^2 \tag{1}$$

Transformation of $x(t)$ using $g(x)$ will generally result in a non-Gaussian signal, $y(t)$, whose statistics vary according to the particular values of the coefficients a, b, and c. The output waveform, $y(t)$, will have a PDF that is given by

$$\text{PDF}(y) = \frac{\text{PDF}(x)}{|dg/dx|} \tag{2}$$

For the special case where $c = 0$, $y(t)$ has Gaussian statistics because the transformation function is no longer nonlinear and a linear transformation (i.e., an additive and/or multiplicative scaling of the time series) of a Gaussian signal yields a Gaussian signal.

One significant step in the simulation process is that of selecting a suitable NTF to achieve the desired probability distribution and moments. Equation (1) was chosen to be the NTF for these jet noise waveform simulations because it was noted from a nonlinear systems text by Bendat [7] that the PDF for a high-amplitude jet noise waveform in [1] is very similar to that of a hardening–softening nonlinear spring. To illustrate, the NTF for a hardening–softening spring may be written as

$$y = g(x) = x + cx^2 \tag{3}$$

and an example PDF for $c = 0.138$ is displayed in Fig. 1. There is notable similarity in the overall shapes between the probability distribution in Fig. 1 and the PDF for the F/A-18E waveform at AB, which is displayed along with an ideal Gaussian curve in Fig. 2. Note further that the AB PDF is comparable to the high-power jet noise PDFs in Figs. 3 and 5 of [1]. These results suggest that Eq. (3) or a similar equation may be an acceptable choice for an NTF to model an asymmetrical jet noise PDF. However, the difficulty with simply using Eq. (3) as the NTF for these simulations is the abrupt truncation of the PDF at negative values of $y(t)$. This truncation is necessary to

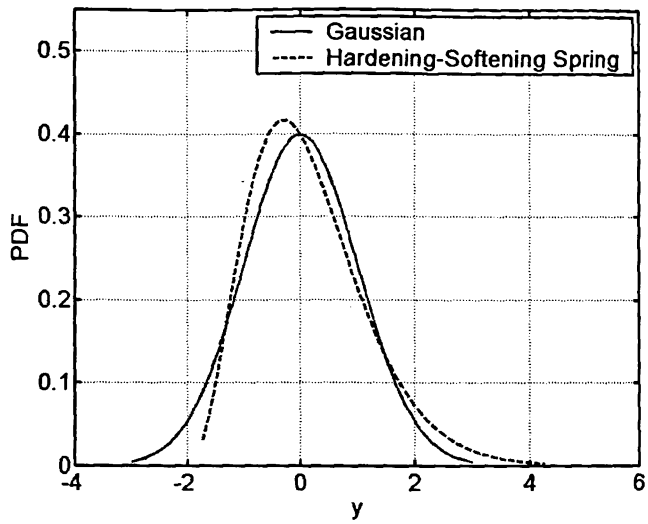

Fig. 1 Probability density functions for a hardening–softening nonlinear spring and a Gaussian distribution. For this example, the coefficient in Eq. (3) is $c = 0.138$ and $|x| \leq 3.0$.

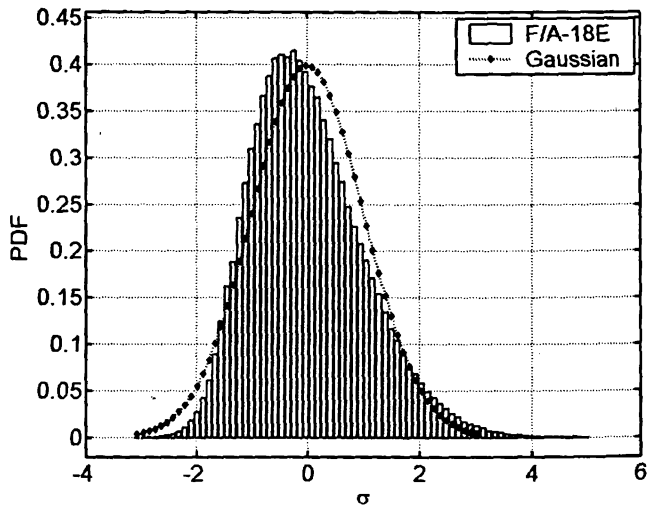

Fig. 2 Probability density function (PDF), shown in terms of number of standard deviations (σ) for the F/A-18E Super Hornet made with the tied-down aircraft at afterburner and at a distance of 18 m. See [3] for additional measurement details. This afterburner PDF, which is compared against an ideal Gaussian distribution, is very similar to that shown by Ffowcs Williams et al. for the Rolls Royce Olympus 593 engine at high power [1]. Note also the similarity between the jet noise PDF and the hardening–softening spring PDF shown in Fig. 1.

maintain a one-to-one relationship between y and PDF(y) as a result of the parabolic nature of the single degree-of-freedom NTF of the hardening–softening spring. Equation (1) is the result of generalizing the parabolic NTF in Eq. (3) to include additional coefficients (degrees of freedom), which has the effect of removing the abrupt truncation in Fig. 1 and creating a more realistic negative tail to the PDF, as will be shown later.

In addition to the quadratic NTF, a range of alternative NTFs has also been studied, including a cubic polynomial of the form

$$y = a + bx + cx^2 + dx^3 \tag{4}$$

and a generalized sigmoidal function, which is expressed as

$$y = a + \frac{b}{1 + e^{-c(x-d)}} \tag{5}$$

The functions found in Eqs. (4) and (5) may initially appear to be more plausible candidates than the quadratic NTF in Eq. (1) because they both can yield quadraticlike NTFs, but have four variable coefficients, rather than only three. This additional coefficient could

potentially be important because specification of M, V, S, and K to find the three coefficients in Eq. (1) represents an overdetermined system with four constraints and only three unknowns. However, it was found when Eqs. (1), (4), and (5) were, respectively, implemented in the algorithm outlined below that the cubic and sigmoidal NTFs generally did not yield improved results and the outputs were extremely sensitive to initial parameter choices in the iterative scheme used to determine NTF coefficients. This is probably because dg/dx for Eqs. (4) and (5) is itself a nonlinear function, whereas dg/dx is linear for Eq. (1). The remainder of this section is dedicated to descriptions of the creation of $x(t)$ and of the iterative coefficient selection process.

Equation (1) appears to closely approximate the statistical behavior of the measured AB jet noise for appropriate choices of coefficients a, b, and c. Before use of an iterative scheme to select these coefficients, a statistically Gaussian white noise waveform is first created and filtered so as to possess a nearly identical power spectrum as the actual AB data. Although waveform filtering is perhaps more traditionally carried out in the time domain via convolution of the waveform with an appropriate impulse response function (see [8] for an example), for this work, filtering was carried out in the frequency domain by: 1) Fourier transforming the waveform, 2) multiplying the white Fourier spectrum by the square root of the power spectrum of the AB data, 3) performing an inverse Fourier transform, and 4) scaling the filtered Gaussian waveform to ensure that it possessed the same variance (and overall sound pressure level) as the AB time series. Modification of a Gaussian waveform's spectral shape does not appreciably change its statistics, provided that the new spectral shape is sufficiently broadband (as is jet mixing noise). The resultant filtered waveform, $x(t)$, is then transformed according to Eq. (1) when the desired coefficients are found.

The coefficients are derived via iterative minimization of a quadratic error or cost function based on the desired moments of the probability density function of the simulated data, PDF(y), which is calculated according to Eq. (2). For example, given a zero-mean process ($M = 0$) and specified desired values for the variance, skewness, and kurtosis, the error function E may be written as

$$E_i = M_i^2 + (V_i - V)^2 + (S_i - S)^2 + (K_i - K)^2 \tag{6}$$

where the subscript i represents the values of the moments of PDF(y) for the ith iteration. After PDF(y) is calculated for each iteration, the area under its curve, A, is calculated by numerically evaluating the integral

$$A = \int_{-\infty}^{\infty} \mathrm{PDF}(y)\,dy \tag{7}$$

The moments M_i, V_i, S_i, and K_i required to evaluate the cost function are then calculated by numerical evaluation of

$$M_i = \frac{1}{A}\int_{-\infty}^{\infty} y\mathrm{PDF}(y)\,dy \tag{8}$$

$$V_i = \frac{1}{A}\int_{-\infty}^{\infty} (y - M_i)^2\mathrm{PDF}(y)\,dy \tag{9}$$

$$S_i = V_i^{-3/2}\frac{1}{A}\int_{-\infty}^{\infty} (y - M_i)^3\mathrm{PDF}(y)\,dy \tag{10}$$

and

$$K_i = V_i^{-2}\frac{1}{A}\int_{-\infty}^{\infty} (y - M_i)^4\mathrm{PDF}(y)\,dy \tag{11}$$

The MATLAB® function "fminsearch," which performs unconstrained nonlinear optimization on a multivariable scalar function [9], is used to find the values of a, b, and c of the NTF that minimizes E. The results of the simulation process are now shown and discussed.

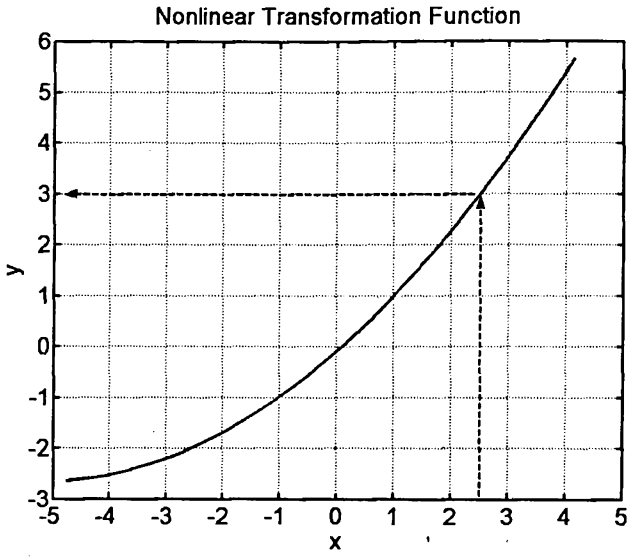

Fig. 3 Quadratic nonlinear transformation function used to transform a Gaussian waveform to a non-Gaussian waveform with positive skewness. The dashed lines demonstrate how the nonlinear transformation occurs. In this case, $x = 2.5$ results in $y = 3.0$.

III. Simulation Results and Playback

A. Results

The preceding theory has been used to create simulated versions of the F/A-18E AB and Mil waveforms. To demonstrate the salient point of this research, only one example will be described in detail. Because the AB skewness is significantly greater than that of the Mil waveform, and therefore farther from the Ffowcs Williams et al. threshold, the AB results have been selected for presentation.

After the nonlinear transformation process described in Sec. II was carried out to create a waveform that simulated the recorded AB waveform, minor differences between M and V for $y(t)$ and the AB waveform were removed by subtracting off the mean and scaling the waveform to match the overall sound pressure level of the measured F/A-18E waveform [5] (150 dB re 20 μPa). The NTF used to generate the simulated non-Gaussian waveform is shown in Fig. 3, where x and y are normalized to $\sigma = 1$. The parabolic shape in Fig. 3 is obtained by substituting $a = -0.0959$, $b = 0.9911$, and $c = 0.0960$ into Eq. (1). The dashed lines are shown as an example of how the transformation from a Gaussian to a non-Gaussian waveform occurs. In the example, an input $x = 2.5$ yields the output $y = 3.0$. The values of S and K for $x(t)$, $y(t)$, and the AB data are displayed in Table 1. As a result of the nonlinear transformation process, the non-Gaussian simulation waveform has skewness and kurtosis values that are very close to the actual AB data.

In Fig. 4, the initial Gaussian, simulated non-Gaussian, and actual AB waveforms are displayed on an expanded scale. Passage of the Gaussian waveform through the NTF yields a simulated waveform that has an overall appearance that is very similar to the AB data in terms of observable skewness. The Gaussian waveform is symmetric about zero, whereas the non-Gaussian simulation possesses an asymmetry that is similar to the AB waveform. The power spectral densities for these waveforms are displayed in Fig. 5. The power

Table 1 Skewness (S) and kurtosis (K) values for the Gaussian, non-Gaussian simulation, and AB waveforms. The Gaussian waveform is very close to that of ideal Gaussian behavior, for which $S = 0$ and $K = 3$

Waveform	S	K
Gaussian	0.02	3.01
Simulation	0.57	3.39
AB Data	0.60	3.40

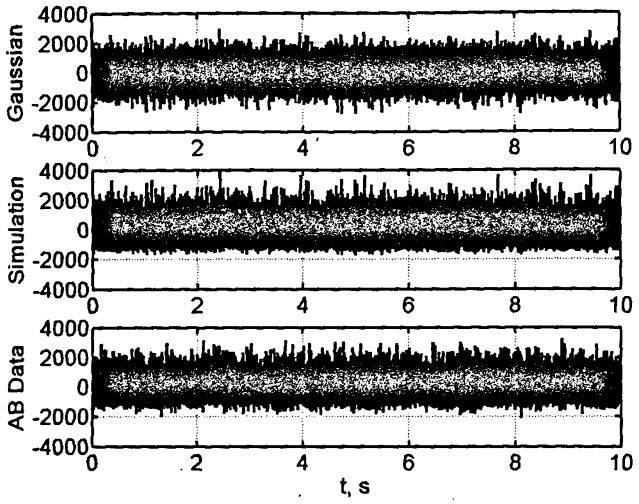

Fig. 4 Gaussian, simulated non-Gaussian, and AB waveforms. All three waveforms are zero-mean signals and have the same variance. The Gaussian waveform has zero skewness, whereas the simulated and AB waveforms have significant positive skewness.

spectral density for the Gaussian noise waveform is essentially equal to that of the measured AB data because of the initial filtering of the white noise signal. The spectral density of the non-Gaussian simulated waveform is slightly distorted at low frequencies as a result of the nonlinear transformation, but generally matches the overall spectrum quite well. In other words, the NTF does not significantly modify the spectral shape in creating $y(t)$ from $x(t)$, but it does significantly impact the waveform statistics. This finding is in accordance with the initial observation by Ffowcs Williams et al. that crackle (or waveform skewness) is indiscernible in power spectral calculations [1].

As Table 1 indicates, the skewness and kurtosis of the simulated waveform are very close to the actual values of the AB waveform. Furthermore, as discussed, the waveforms have been scaled to have an identical mean and variance. However, this level of similarity does not necessarily guarantee that the PDFs of the two waveforms will be the same because no constraints have been placed on any moments greater than order four. To show that the overall statistical behavior of the two waveforms is largely determined by these four moments, the PDFs of the simulated and AB waveforms are shown in Fig. 6 along with the Gaussian PDF of $x(t)$. To completely compare the simulated and AB PDFs, Figs. 6a and 6b, respectively, have linear and logarithmic ordinates. The linear scale emphasizes behavior near the center of the distribution whereas the logarithmic scale is helpful in comparing the tails of the distributions. Examination of Fig. 6a

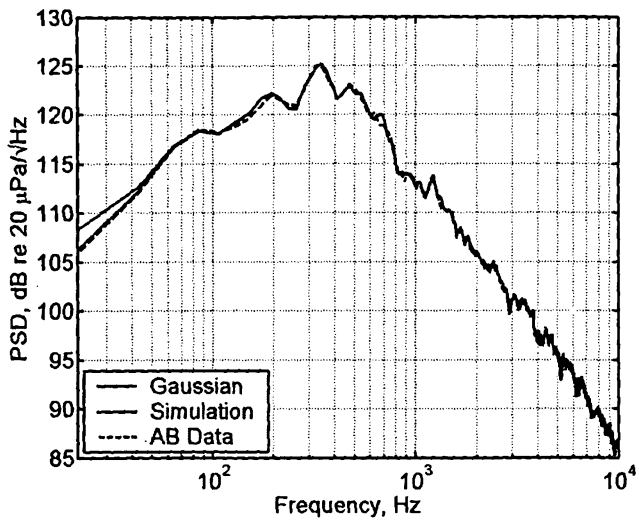

Fig. 5 Power spectral densities of the Gaussian, non-Gaussian simulated, and AB waveforms. Except at very low frequencies, the Gaussian and simulated spectral densities overlay that of the AB data.

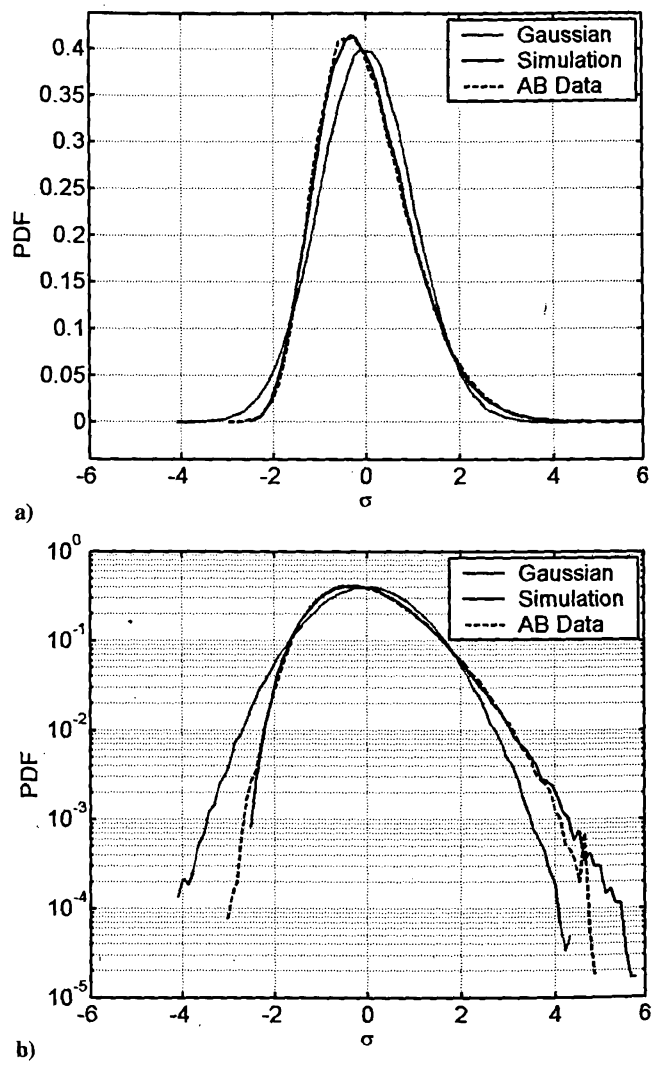

Fig. 6 Probability density functions of the Gaussian, non-Gaussian simulated, and AB waveforms. The PDFs are represented on a linear scale in a) and on a logarithmic scale b).

reveals that the simulated PDF matches that of the AB waveform very closely over the high-probability regions of the distribution. As shown in Fig. 6b, there are differences between the two PDFs in both the positive and negative tail regions, but only where the probability of occurrence is very low. Specifically, the simulated PDF only begins to diverge from the AB PDF at the positive and negative tails when the probability is nearly 2 orders of magnitude below the maximum probability.

B. Playback of Waveforms

The previous study by Ffowcs Williams et al. [1] indicates that because $S = 0.57$ for the simulated waveform, $y(t)$, and $S = 0.02$ for the Gaussian waveform, $x(t)$, crackle should be present in $y(t)$ but not in $x(t)$. Although direct playback of the waveforms is not possible in this article, the waveforms were directly embedded as hyperlinks into a previous AIAA conference paper [10] version of this article. The waveforms may also be found at the Internet URL[¶] or may be obtained via email.

Listening to both the Gaussian and non-Gaussian simulated waveforms demonstrates there is little, if any, perceived difference between the simulated and Gaussian waveforms and nothing in the simulated waveform that has a cracklelike quality. This result contradicts the distinct crackle threshold suggested by Ffowcs Williams et al. in that $S = 0.57$ but does not crackle. This simulation

[¶]The waveforms may be found at K. L. Gee's faculty website: http://www.physics.byu.edu/faculty/gee/crackle.aspx. Note that because this is not an archived website, the link may occasionally change. However, the waveforms may be obtained by emailing any of the authors.

also indicates there is more to the perceptual phenomenon of crackle than simply significant positive skewness. The reasons for the absence of crackle from the highly skewed simulated waveform are now explored.

IV. Waveform Time Derivative Analysis

Because there are extreme perceptual differences between the non-Gaussian simulated and the recorded AB waveforms, the waveforms themselves merit a closer look. Displayed in Fig. 7 are short segments of the Gaussian, simulated, and AB waveforms. A comparison of the Gaussian and simulated waveforms shows in more detail the nonlinear transformation process that yields the skewed waveform. A comparison between the simulated and AB waveforms reveals a significant difference between the simulated and actual data. The AB waveform tends to "lean" one direction and contains some very sharp pressure rises, whereas the simulated waveform does not. It is noted that these characteristics of the AB waveform are consistent with descriptions of crackling waveforms provided by Ffowcs Williams et al. [1] and Krothapalli et al. [2]. The lack of crackle in the simulated waveform appears to be related to the fact that these features are not present in the simulated waveform.

The AB and non-Gaussian simulated waveforms have essentially the same spectrum (see Fig. 5) and PDF (see Fig. 6) but are perceived to be very different because of the sharp shocklike pressure rises that are present in the AB waveform but not in the simulated waveform. This difference may be better investigated via calculations and statistical analysis of the time derivatives of the waveforms, a data processing technique that is largely due to McInerny (e.g., see [4,11,12]). Figure 8 displays the time derivatives of the waveform segments shown previously in Fig. 7. The derivatives, which are normalized to $\sigma = 1$ for visualization purposes, have been estimated via a simple first-order forward difference because more accurate derivative estimation methods have smoothness constraints that are violated here. This figure reveals a marked difference between the non-Gaussian simulated waveform and the AB data. The sharp pressure rises present in the AB waveform lead to large positive spikes in the time derivative estimate that are not present in the simulated waveform.

The differences in the time derivatives between the Gaussian, non-Gaussian simulated, and AB waveforms are better quantified in terms of their PDFs and associated moments. The PDFs of the time derivatives are shown on both linear and logarithmic scales in Figs. 9a and 9b. These figures reveal more clearly the dramatic disparity between the time derivatives of the AB and simulated waveforms. The simulated waveform differs only slightly from Gaussian behavior, whereas the AB waveform is significantly non-Gaussian and has a large positive tail that is formed by the steep rise portions of the waveform and continues out to approximately 28σ.

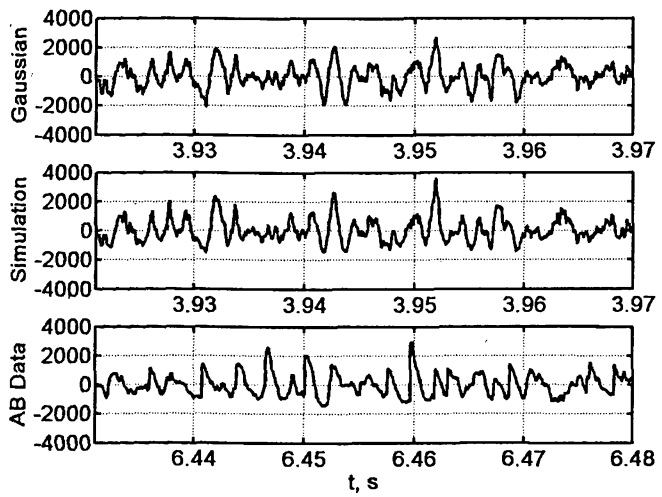

Fig. 7 Segments of the Gaussian, non-Gaussian simulation, and AB waveforms. The compressive portions of the AB waveform are generally much more shocklike than the non-Gaussian simulation. See the text in Sec. IV for further explanation and discussion.

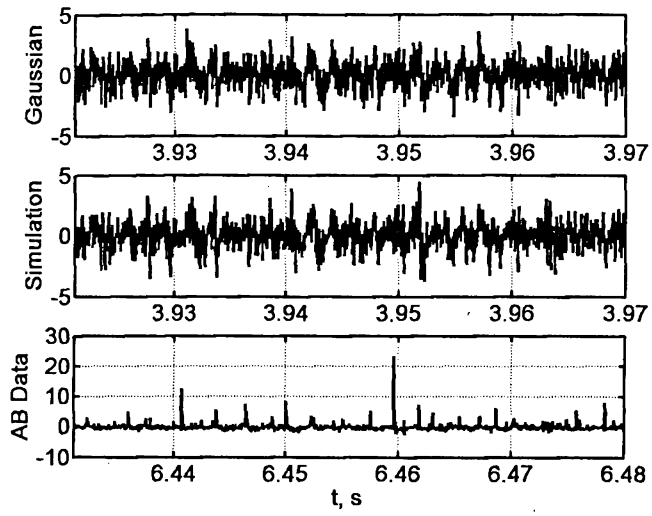

Fig. 8 Normalized time derivative estimates for the acoustic pressure waveform segments displayed in Fig. 7. The pressure time derivatives are normalized by their respective standard deviations. Note that the abscissa for the AB data is significantly different than those of the simulation and Gaussian time derivatives.

These differences are quantified with S and K calculations for the Gaussian, non-Gaussian simulation, and AB waveforms in Table 2. The derivative of the simulated waveform has zero skewness and somewhat non-Gaussian kurtosis, whereas the AB data reveal extreme non-Gaussian behavior that appears to be directly related to the perception of crackle in actual high-amplitude jet noise.

V. Discussion and Conclusions

This investigation of the perception of crackle gives rise to a number of points of discussion and conclusions. First of all, despite the fact that the simulation process yields a simulated waveform that is virtually the statistical equivalent to the AB waveform, the results of this simulation demonstrate that skewness is not sufficient by itself to cause a listener to perceive crackle. The analysis of the time derivatives of the waveforms indicates that shocklike features must be present in the time waveform. Ffowcs Williams et al. [1] discussed the fact that the intense compressive portions of the waveform usually had short rise times and further concluded that the "physical feature of a sound wave that gives rise to the readily identifiable subjective impression of 'crackle' is shown to be the sharp shocklike compressive waves that sometimes occur in the wave form."

Although this physical interpretation does, in fact, appear to be correct, positive waveform skewness does not account for how quickly or how slowly pressure fluctuations occur, but rather only that pressure values occur in a waveform with some asymmetric probability. Ffowcs Williams et al. understood crackle and positive waveform skewness to be synonymous [1]; however, this appears not to be the case. This leads to the conclusion that if the sharp pressure changes account for the subjective impression of crackle, use of the time derivative of the waveform, rather than the waveform itself, to quantify the phenomenon of crackle is merited. This result corroborates the findings of McInerny [4], who concluded from her rocket noise study that the skewness of the time derivative of the waveform was a more sensitive indicator of the waveform's shock content than the skewness of the waveform itself. Although the skewness of the time derivative may, in fact, be an appropriate quantifier of crackle, additional research should be conducted to further study its suitability.

Table 2 Skewness (S) and kurtosis (K) values for the time derivatives of the Gaussian, non-Gaussian simulation, and AB waveforms

Waveform	S	K
Gaussian	0.00	3.00
Simulation	0.00	3.40
AB Data	5.59	67.3

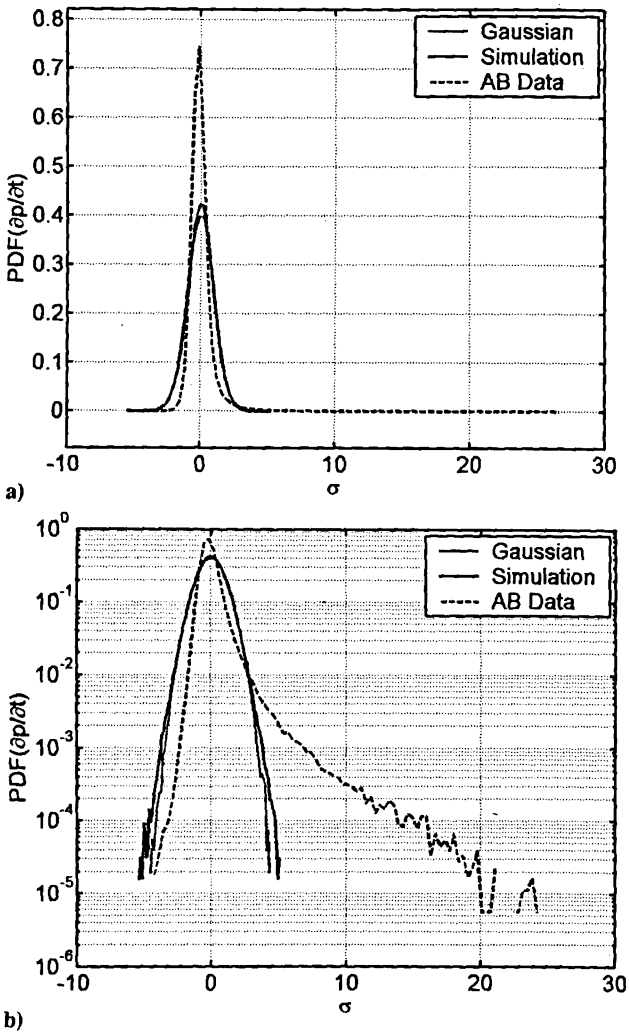

Fig. 9 Probability density functions of the time derivatives of the Gaussian, non-Gaussian simulated, and AB waveforms. The PDFs are represented on a linear scale in a) and on a logarithmic scale b). Note that discrete occurrences in the AB waveform's PDF continue out to 28 standard deviations (σ).

This conclusion regarding an appropriate metric for quantifying crackle leads to another point of discussion, that of similarity between perceived "nonlinearity" and perceived crackle. As mentioned in the Introduction, a recent study by Gee and Sparrow [6] shows that a waveform that is nonlinearly propagated numerically can take on an impulsive quality that could be potentially perceived as cracklelike. This occurs despite the fact that the waveform's skewness may be essentially zero [13]. Furthermore, the perceived difference between linearly and nonlinearly propagated signals is significant in that the linear waveform does not have this impulsive quality, but this difference is not evident in the nearly identical waveform PDFs. There is, however, an unmistakable difference in the PDFs of the waveforms' time derivatives, which indicates that the impulsive quality to the nonlinearly propagated waveform appears to be linked to waveform steepening and acoustic shock formation in the course of propagation. A crackling acoustic waveform in the near field of a jet also possesses shocklike structures that are evident in the PDF of the waveform time derivative and appear to be critical to the perception of crackle. Any further connection between the two phenomena remains to be explored.

An additional study that merits mention is that by Downing et al. [12], in which high-bandwidth measurements of military jet aircraft flyovers were analyzed. The results revealed a clear relationship between overall sound pressure level (OASPL) and skewness of the time derivative of the waveform. As OASPL increased, so did the derivative's skewness. On the other hand, only a weak relationship was found between OASPL and skewness of the waveform itself. An extension of the study by Downing et al. would be to perform listening tests with the flyover waveforms to determine if the relative contribution of the cracklelike phenomenon to overall annoyance also increases as a function of OASPL or if it remains relatively constant.

One final point of discussion regards the ability to generate a simulated jet noise waveform that does, in fact, create the perception of crackle. This may be possible with the nonlinear transformation process described in Sec. II for an appropriate choice of a nonlinear transformation function that can yield an extremely non-Gaussian PDF as is shown in Fig. 9. Refinement of such a simulation process could greatly reduce the data storage requirements for total jet noise source characterization because entire waveforms could be replaced by power spectra and a few statistical measures that could then be used to create statistically and perceptually equivalent waveforms.

Acknowledgments

K. L. Gee and V. W. Sparrow acknowledge the support of the Strategic Environmental Research and Development Program and Wyle Laboratories. A. A. Atchley and T. B. Gabrielson acknowledge the support of the Office of Naval Research. The authors are also indebted to D. O. Smallwood of Sandia National Laboratories for helpful discussions and example code related to non-Gaussian waveform simulation.

References

[1] Ffowcs Williams, J. E., Simson, J., and Virchis, V. J., "'Crackle': An Annoying Component of Jet Noise," *Journal of Fluid Mechanics*, Vol. 71, No. 2, 1975, pp. 251–271.

[2] Krothapalli, A., Venkatakrishnan, L., and Lourenco, L., "Crackle: A Dominant Component of Supersonic Jet Mixing Noise," AIAA Paper 2000-2024, June 2000.

[3] Petitjean, B. P., and McLaughlin, D. K., "Experiments on the Nonlinear Propagation of Noise from Supersonic Jets," AIAA Paper 2003-3127, May 2003.

[4] McInerny, S. A., "Launch Vehicle Acoustics Part 2: Statistics of the Time Domain Data," *Journal of Aircraft*, Vol. 33, No. 3, 1996, pp. 518–523.

[5] Gee, K. L., Gabrielson, T. B., Atchley, A. A., and Sparrow, V. W., "Preliminary Analysis of Nonlinearity in Military Jet Aircraft Noise Propagation," *AIAA Journal*, Vol. 43, No. 6, 2005, pp. 1398–1401.

[6] Gee, K. L., and Sparrow, V. W., "Quantifying Nonlinearity in the Propagation of Noise from Military Jet Aircraft," *Proceedings of Noise-Con 05* [CD-ROM], edited by J. S. Bolton, P. Davies, and G. C. Maling, Jr., Institute of Noise Control Engineering of the USA, Washington, D. C., 2005, Paper nc05_194.

[7] Bendat, J. S., *Nonlinear Systems: Techniques and Applications*, Wiley, New York, 1998.

[8] Harper-Bourne, M., "On Modelling the Acoustic Forcing Functions of the Near-Field Noise of High-Speed Jets," AIAA Paper 2005-2997, May 2005.

[9] MATLAB, Release 14, The Mathworks, Inc., Natick, MA, 2006.

[10] Gee, K. L., Sparrow, V. W., Atchley, A. A., and Gabrielson, T. B., "On the Perception of Crackle in Noise Radiated by Military Jet Aircraft," AIAA Paper 2006-2530, May 2006.

[11] McInerny, S. A., and Olcmen, S. M., "High-Intensity Rocket Noise: Nonlinear Propagation, Atmospheric Absorption, and Characterization," *Journal of the Acoustical Society of America*, Vol. 117, No. 2, 2005, pp. 578–591.

[12] Downing, J. M., Hobbs, C. M., James, M. J., McInerny, S. A., and Hannon, M., "Metrics That Characterize Nonlinearity in Jet Noise," *Innovations in Nonlinear Acoustics: Proceedings of 17th International Symposium on Nonlinear Acoustics*, edited by A. A. Atchley, V. W. Sparrow, and R. M. Keolian, American Institute of Physics Conference Proceedings Series, Vol. 838, AIP, Melville, NY, 2006.

[13] One case considered in the study by Gee and Sparrow [6] dealt with the numerical propagation of an initially Gaussian, high-amplitude noise waveform. The statistics of the waveform itself do not change remarkably when nonlinearly propagated numerically. On the other hand, the statistics of the waveform time derivative change considerably as acoustic shocks form and a cracklelike quality of the noise is heard when the waveform is played back. The waveform is embedded as a hyperlink in the electronic version of [6].

B. Balachandran
Associate Editor